Available online at www.sciencedirect.com
SCIENCE DIRECT
Diamond & Related Materials 13 (2004) 1923–1929
DIAMOND AND RELATED MATERIALS
www.elsevier.com/locate/diamond

Self-assembly of uniform carbon nanotip structures in chemically active inductively coupled plasmas

Z.L. Tsakadze[a], K. Ostrikov[a,b,*], J.D. Long[a], S. Xu[a]

[a] Plasma Sources and Applications Center, NIE, Nanyang Technological University, 637616, Singapore
[b] School of Physics, The University of Sydney, Sydney NSW 2006, Australia

Received 19 September 2003; received in revised form 10 June 2004; accepted 16 June 2004
Available online 20 July 2004

Abstract

Self-assembly of carbon nanotip (CNTP) structures on Ni-based catalyst in chemically active inductively coupled plasmas of CH_4+H_2+Ar gas mixtures is reported. By varying the process conditions, it appears possible to control the shape, size, and density of CNTPs, content of the nanocrystalline phase in the films, as well as to achieve excellent crystallinity, graphitization, uniformity and vertical alignment of the resulting nanostructures at substrate temperatures 300–500 °C and low gas pressures (below 13.2 Pa). This study provides a simple and efficient plasma-enhanced chemical vapor deposition (PECVD) technique for the fabrication of vertically aligned CNTP arrays for electron field emitters.

Keywords: Nanostructures; Nanoparticles; Plasma CVD; Etching; Surface microscopy; Surface structure; Electronic device structures

1. Introduction

Carbon-based nanostructures (CNSs) have been of a remarkable recent interest due to their unique physico-chemical properties that make them attractive for a number of challenging applications ranging from guest molecule storage elements and active media for various chemical reactions to functional elements of data storage and electron field emitting (EFE) optoelectronic devices [1–5]. However, the nanostructures have to satisfy a number of criteria to be suitable for most of the existing and future applications. For example, the EFE applications require a specific shape and size of the individual CNSs, high degree or positional uniformity and vertical alignment of CNSs over large areas, high sp^2 content, excellent crystallinity, and several others [6]. Furthermore, a successful integration of the CNSs into microelectronic devices requires low temperatures and pressures during the chemical vapor deposition (CVD) compatible with the standards of the integrated circuit fabrication processes. For example, the process temperatures must be well below the melting points of the metallic interconnects in the Ultra Large Scale Integrated circuits. Most of the existing CVD methods employing a thermal decomposition (typically in the 800–1200 °C range) of hydrocarbons [7] apparently do not meet the above requirement.

Recently, several plasma-enhanced CVD (PECVD) techniques have been successfully employed for the synthesis of various carbon nanostructures at essentially lower (500–700 °C) sample temperatures [8–12]. A number of elementary processes (e.g. electron-impact dissociation and heavy particle collisions) in the plasma facilitate the dissociation of the hydrocarbon feedstock gas. Meanwhile, intense fluxes of ions and neutrals contribute to the activation of the catalyst layers via a number of physical sputtering (PS) and reactive chemical etching (RCE) processes. The catalyst-coated substrates are usually thermally activated through the external heating (up to 500–700 °C) of the sample supporting surfaces (e.g. sample holders or electrodes). However, at these growth temperatures large amounts of amorphous carbon (a-C) compromise the growth of the nanostructured phase and cause problems in device fabrication and operation [13].

* Corresponding author. Plasma Sources and Applications Center, NIE, Nanyang Technological University, NIE, 1 Nanyang Walk, Singapore 637616, Singapore. Tel./fax: +65-6790-3931.
E-mail address: kostrikov@nie.edu.sg (K. Ostrikov).

0925-9635/$ - see front matter © 2004 Elsevier B.V. All rights reserved.
doi:10.1016/j.diamond.2004.06.010

In this article, we report on the growth and electron field emission properties of the vertically aligned carbon nanotip (CNTP) arrays synthesized in high-density, low-frequency (~460 kHz) inductively coupled plasmas (LF ICPs) in a low-pressure (~11.22 Pa) regime. Excellent uniformity of CNTP structures is achieved without the use of any pre-patterned substrates and nano-lithography techniques. Using the LF ICP technique, it appears possible to suppress the amorphous phase and enhance the preferential growth of the crystalline nanostructured phase at low growth temperatures of 300–350 °C. Furthermore, the CNTP structures (also termed "needle-like structures" here) feature elevated content of sp^2-bonded carbon, pronounced crystallinity, and target the electron field emitting applications.

2. Experimental details

The plasma of the low-pressure methane/hydrogen/argon gas mixtures sustained in a low-frequency (~460 kHz) inductively coupled plasma reactor [14] with an external flat spiral inductive coil (delivering RF power ~2 kW to the cylindrical reactor chamber with the diameter of 0.32 m and length of 0.23 m) were used in the PECVD process. Lightly doped Si(100) wafers (usually 2×2 cm^2) with a thin (~30 nm) Ni-based catalyst layer, pre-deposited in a ultra-high vacuum sputtering facility, were used as substrates. High-purity (99.99%) working gases Ar, H_2, and CH_4 were introduced into the chamber sequentially. First, 30-min conditioning of the substrates was performed in pure Ar at 7.9 Pa. Subsequently, a pure hydrogen etching gas (partial pressure 2.24 Pa) was added in order to trigger the fragmentation of the thick catalyst layer. The etching process in $Ar + H_2$ mixture typically lasted approximately 20 min. After that, a carbon-bearing gas CH_4 (partial pressure 1.05 Pa) was added to the above gas mixture. The actual PECVD process duration was approximately 40 min. Low-pressure (11.22 Pa) plasma discharges were operated in the high density ($n_{e,i} \sim 10^{12}$ cm^{-3}) electromagnetic (H) mode of low-frequency inductively coupled plasmas [14] sustained with RF power densities of $(0.9–1.1) \times 10^5$ W/m^3. Here, n_e and $n_{,i}$ denote the electron and ion number densities, respectively.

A specially designed substrate holder equipped with an insulated heating element encapsulated in the substrate-holding assembly, digital temperature controller and a thermocouple was electrically insulated from the grounded chamber and externally biased with a negative DC potential. Using this arrangement, the CNTP growth regime in our experiments is thus termed as a Temperature-Controlled Growth (TCG) regime with the external control and stabilization of the substrate temperature. To enhance the ion fluxes onto the samples, the top surface of the substrate holder was positioned in the area of the maximal electron/ion density in the plasma reactor.

Field Emission Scanning Electron Microscopy (FE SEM), X-ray diffraction (XRD, CuKα source with 0.154 nm X-ray wavelength) and Raman (Ar^+ laser, 514.5 nm spectral line) spectroscopy were used to characterize the morphology, crystalline structure and chemical states of the needle-like structures. Further details of the operation, plasma parameters and applications of the LF ICP reactor can be found elsewhere [14].

3. Experimental results

The CNTP growth experiments were started with a pre-selected substrate temperature $T_s = 500$ °C and an optimized DC substrate bias V_s. The best results for the area density of CNTPs were achieved at the DC substrate bias $V_s = -80$ V. It was observed that a minimum DC bias V_{min} is required to trigger the nanostructure growth. In our experiments, V_{min} was approximately −50 V, which is much lower than reported previously under similar conditions [11].

At zero bias (Fig. 1(a)), only massive nanoparticle agglomerates that partially cover the surface can be seen and no other CNSs are observable. When the substrate bias is increased to $V_b = -50$ V, the surface morphology comprises irregular-shaped structures (ISS), presumably formed from the nanoparticle agglomerates, and individual carbon nanotips (typically 10–20 nm in diameter and 50–70 nm in height) rarely distributed over the surface between the ISSs (Fig. 1(b)). Further increase of the bias yields higher surface densities of the needle-like structures and reduces the amount of the nanoparticle agglomerates on the surface. We note that at fixed substrate temperatures the density of the nanotips strongly depends on the bias. Indeed, a modest change of V_b to −60 V leads to a pronounced increase of the number of CNTPs per unit area

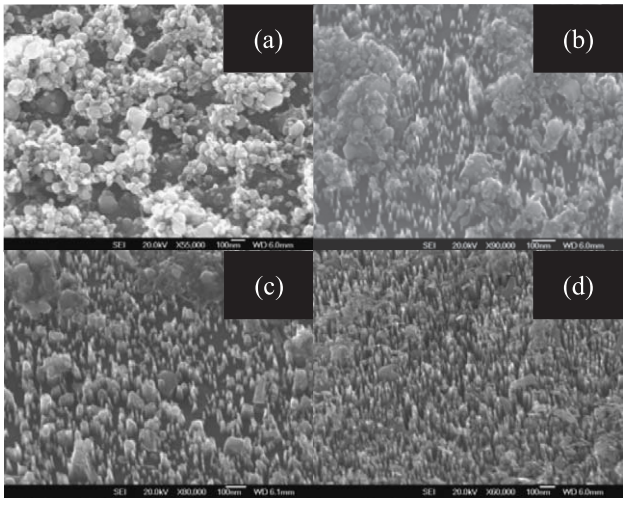

Fig. 1. SEM micrographs of carbon nanostructures grown at $T_s = 500$ °C and different DC biases. Images (a)–(d) correspond to $V_b = 0$, −50, −60, and −80 V, respectively.

(Fig. 1(c)). From this point of view, the best results were achieved applying the DC bias $V_b = -80$ V (Fig. 1(d)). In this case the nanotips almost entirely cover area between the ISSs; however, their ordering still remains quite poor. At the same time, as will be shown below by Raman spectrometry (presence of a strong photoluminescence background), there is a notable content of the amorphous carbon (a-C) phase in the films.

In an attempt to inhibit the deposition of amorphous carbon and minimize the CNTP deposition temperature, further experiments were performed at lower T_s (300–400 °C). The results of the nanostructure growth in this temperature range and the same DC bias ($V_b = -80$ V) are shown in Fig. 2. One can notice that at 400 °C (Fig. 2(a)) the ISSs and self-organized nanotip "bundles" are smaller as compared to the case shown in Fig. 1(d), although their presence in the film is still quite high. However, a further decrease of the substrate temperature to 350 °C and 300 °C makes a drastic change to more regular and well-resolved nanostructures with the CNTPs (20–30 nm in diameter and 140–160 nm in height) (Fig. 2(b) and (c)). More importantly, ordering and uniformity of the CNTP structures (critical factors in the EFE development) improved much as compared to the cases with T_s>400 °C. The estimated value of the film thickness is ~0.5 μm. The areal density of the individual nanostructures was also affected by this change in the temperature, with the average number of CNTPs per linear micron being approximately 32–47. It is remarkable that the growth mode of the films features a high uniformity over the entire surface of the samples (up to approximately 10 cm^2 in our experiments).

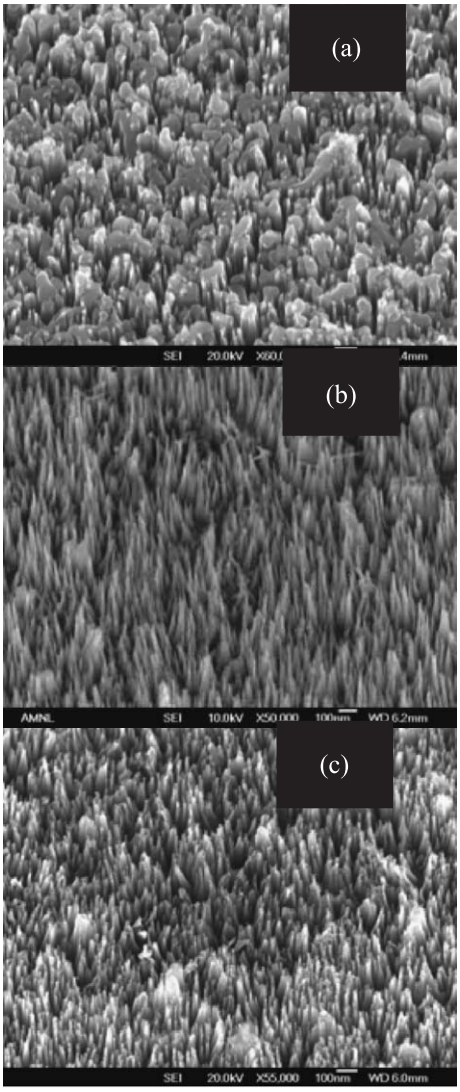

Fig. 2. FE SEM images of CNTP structures grown at $V_b = -80$ V and $T_s = 400$ (a), 350 (b), and 300 °C (c). Other parameters are the same as in Fig. 1.

From Fig. 2(b) and (c) one can conclude that an excellent uniformity of the CNTPs can be achieved in the low-pressure (<13.2 Pa) range suitable for microelectronic manufacturing. Furthermore, the ordering of the nanostructures is quite sensitive to the changes in the substrate temperature. We note that the process temperatures and gas pressures in our growth experiments are noticeably lower than in many relevant plasma-based methods of fabrication of various carbon-based nanostructures [8–12,15].

The films feature high degree of crystallization, which is evidenced by well-resolved peaks in the XRD spectra shown in Fig. 3(a). It is seen that the intensities of most of the diffraction peaks vary with the decrease of the substrate temperature from 500 to 300 °C, which indicates on the changes in the preferential crystal growth direction with T_s. It is interesting that the XRD spectrum of the films grown at 300 °C (curve 1 in Fig. 3(a)) features several broadened peaks in the range of $2\Theta = 33–37°$ indicating on the presence of nano-sized crystals [16] otherwise not present at other temperatures. The origin of the nano-crystals can be attributed to the diffusion properties of the Ni-based catalyst layer. Specifically, at the temperatures above 300 °C, the diffusion of Ni into Si (leading to the formation of a silicide $NiSi_x$) is inhibited, which results in an excellent fragmentation of the Ni-based layer into nano-sized particles [10]. Thus, the efficient suppression of the interface diffusion at T_s<300 °C results in better nanostructuring of the catalyst and hence to the XRD peak broadening clearly seen in Fig. 3(a). On the other hand, since the growth regime of interest here features quite low temperatures (300–400 °C), there is no need for any special barrier interlayer (e.g. SiO_2 or TiN [17]) that can adversely affect the adhesion properties of the nanostructured film.

Raman spectra in Fig. 3(b) show two distinct peaks. Specifically, the tangential C–C stretching mode corresponding to the G peak at approximately 1580 cm^{-1} is attributed to the crystalline graphite, whereas the D peak at approximately 1350 cm^{-1} is attributed to the disorder-induced (e.g. due to the presence of defects in curved graphite

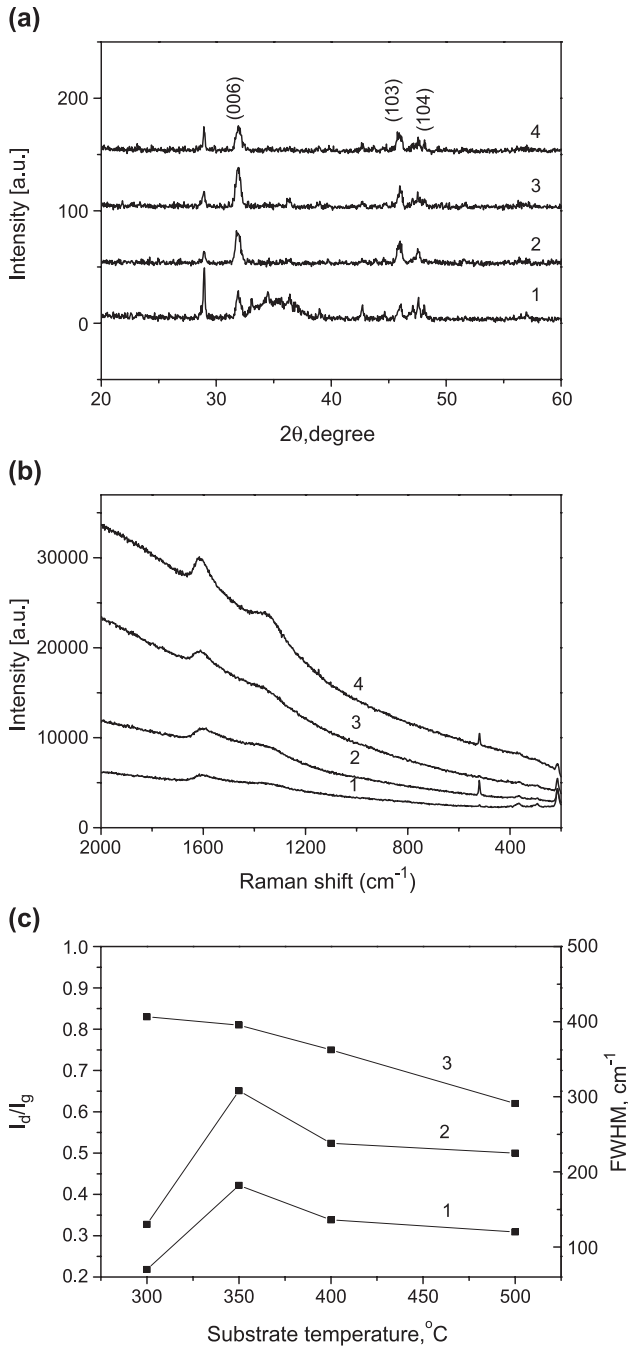

Fig. 3. (a) XRD and (b) Raman spectra; (c) FWHM of the D (curve 1) and G (curve 2) Raman peaks, and I_D/I_G ratio (curve 3) versus substrate temperature for the same parameters as in Fig. 2. Curves 1–4 in figures (a) and (b) are plotted for $T_s = 300$, 350, 400, and 500 °C, respectively.

sheets) Raman scattering from sp^2 carbons. The position and well-defined shape of the D and G peaks point to a well-structured graphitic morphology in the films. We assume that the Raman peak at approximately 211 cm^{-1} can be attributed to the radial breathing mode of the carbon needle-like structures. It is remarkable that the photoluminescence background decreases at lower temperatures, which indicates on the reduced amorphous carbon content [10]. Fig. 3(c) shows the dependence of the ratio of the intensities (I_D/I_G) and the full widths at half maximum (FWHM) of the two important (D and G) peaks on the substrate temperature. When T_s diminishes, the ratio I_D/I_G increases, which indicates on an increase of the number of nano-sized sp^2 clusters that play an important role in the field emission from nanostructured carbons [17]. The observed shapes and frequency shift of the major Raman peaks can be described by the conventional phonon confinement model [18,19]. Using this model, we arrive to the conclusion that the crystallite size is the smallest at $T_s = 350$ °C. It is worth emphasizing that the process temperatures and gas pressures in our carbon nanostructure growth experiments can be remarkably lower than in many existing low-temperature plasma-based methods.

However, lower (~350 °C) substrate temperatures did not lead to the best results for the electron field emission properties. Fig. 4 shows the electron field emission properties of the nanostructured carbon and presents the I–V characteristics of the CNTPs grown at different substrate temperatures. One can see that the needle-like structures grown at low substrate temperatures yield lower field emission currents. The field emission current becomes stronger with an increase of the substrate temperature. The field emission threshold fields are 16.6, 11, and 6.4 V/μm at $T_s = 350$, 400, and 500 °C, respectively. The threshold field is defined as a value of the electric field at which 0.1 μA emission current is obtained over an emitting area of 0.28 cm^2 [20]. From Fig. 4, one can conclude that the rarefied "forest" of carbon nanotips exhibits much higher emission currents than the dense "forests" grown at lower substrate temperatures. These results suggest that the shielding of the electric field between closely packed carbon nanotips in the dense "forest" effectively decreases the field emission from the high aspect ratio nanotips [21]. On the other hand, in the rarefied "nanotip forest" the field shielding effects are

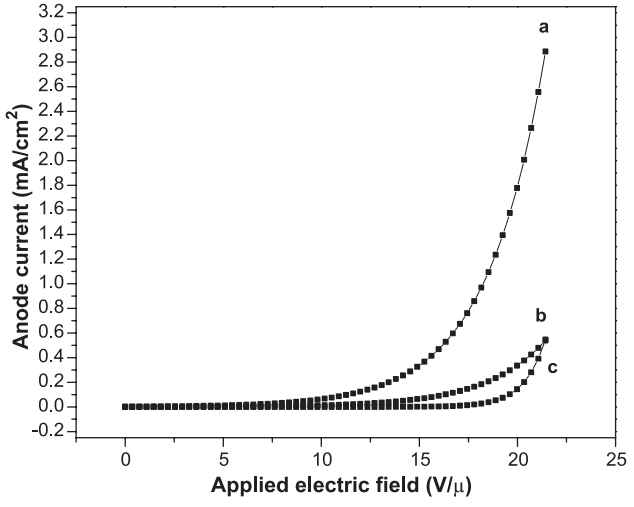

Fig. 4. Field emission characteristics of the samples grown at: (a) 500 °C, (b) 400 °C (multiplied by the factor of 10), and (c) 350 °C (multiplied by the factor of 100).

weaker due to the lower density of the nanostructures. We emphasize that the nanostructured films were remarkably stable in air over long periods of time. In fact, the field emission measurements made after several days or months after the deposition have shown the same results.

4. Discussion

We recall that the growth and field emission properties of highly uniform carbon nanotip structures in low-frequency (~460 kHz) inductively coupled plasmas at low gas pressures (~11.22 Pa) and in the substrate temperature range of 300–500 °C are reported. In Fig. 5, we schematically depict the dynamics of the process of PECVD of the carbon needle-like structures to facilitate the following clarification of the major physico-chemical processes at different stages of the deposition process.

Physically, the resulting surface morphology is strongly affected by the competition of the reactive chemical etching (RCE) of the growth surface by hydrogen and PECVD of a new carbon material from the gas phase. Apparently, the value of the substrate temperature does affect the relative efficiencies of the competing RCE/PS and PECVD processes. At low substrate temperatures (300 °C < T_s < 350 °C) the anisotropic etching prevails and the growth of high-aspect-ratio CNTPs is favored. Furthermore, a variation of the substrate temperature does affect the deposition rate of neutral particles from the ionized gas phase. When T_s increases, the gas heating is more efficient near the deposition surface. Since the gas density in the plasma bulk is higher than near the substrate surface, increasing the substrate temperature effectively elevates the pressure gradient (and hence the diffusion flow of neutrals) in the near-electrode area. On the other hand, our measurements show that the ion current on the substrate remains essentially the same at different temperatures. We can thus relate an overall increase in the deposition rate at higher T_s to the neutral radicals. Meanwhile, higher near-substrate temperature gradients result in stronger thermophoretic (in our case repulsive) forces on the larger (typically in the 10–100 nm range) carbon-based nanoparticles grown in the ionized gas phase [22,23].

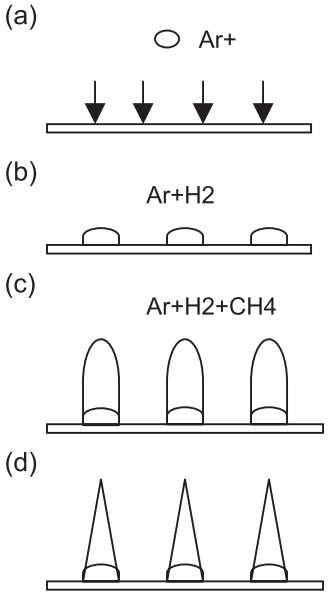

Fig. 5. Schematic diagram of the different stages of the deposition process: (a) surface pre-treatment by argon ions; (b) substrate etching of the catalyzed substrate by hydrogen and formation of islands; (c) growth of CNTP structures; (d) re-shaping of the CNTPs due to the competition between the RCE/PS and PECVD processes.

Films of our interest here can be termed polymorphous in a manner similar to nanostructured silicon-based films [24]. Therefore, the successful growth of the carbon nanostructures does imply a preferential growth of the nanostructured crystal phase and a strongly inhibited growth of the amorphous phase, the latter being an unwelcome component in many device grade films [13]. Physically, in the gas/substrate temperature range of 300–350 °C, the amorphous carbon phase predominantly grows as a result of a chemisorption of CH_3 radicals to hydrogen-terminated carbon surfaces. In this case the carbon dangling bonds can be activated by intense fluxes of the impinging (with the main contribution from Ar^+) ions [25]. Previously, the presence of the amorphous carbon phase on the substrate surface was minimized by a heavy dilution of the carbon-bearing gas (CH_4 or C_2H_2) in the etching gas (e.g. H_2 or NH_3) [13].

Our experiments suggest that the fabrication of carbon needle-like structures does require an optimized DC bias. Specifically, the bias should not be too low to be able to sustain the minimal level of the reactive ion etching and physical ion sputtering to activate the catalyst layer. Furthermore, a DC bias should be strong enough to support the preferential growth direction and vertical alignment of the CNTPs. On the other hand, V_b should not be too high to avoid unwelcome over-activation of the carbon dangling bonds, which is consistent with the previous reports that a minimum (typically approximately −50–100 V) CD bias is required for carbon material to be deposited on the substrate [11]. The minimum DC bias for the CNS growth can be explained by noting that in the dissolution/precipitation growth mechanism, carbonization of nickel on the surface requires external supply of the energy (approx. 9.8 eV), which can be provided as a result of heavy particle collisions involving sufficiently accelerated (by the DC electric field) cations in the near-substrate sheath [15]. When the bias is too large, PECVD of the amorphous carbon (as well as an unwelcome physical sputtering of the growth surface by argon ions) are expected to dominate. On the contrary, under the small bias voltage, the kinetic energy of cations is clearly not enough to carbonize nickel and then the CNTP structures are not formed.

A notable improvement in the ordering of CNTP structures can be attributed to the re-structuring of the self-organized catalyst islands over the deposition area. Indeed,

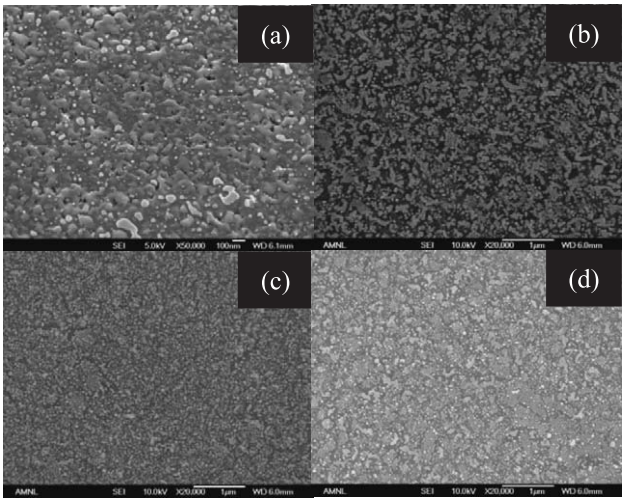

Fig. 6. Same as in Fig. 2 for the surface morphology (top view) of the catalyst layer after the etching stage (a) and CNS growth islands (b)–(d) at $T_s = 500$ (a, b), 350 (c), and 300 °C (d), respectively.

the SEM analysis confirms that the sizes of the growth spots of the carbon nanotips correlate with the sizes of the reorganized (after the RCE stage) catalyst islands (Fig. 6(a) and (b)) and become smaller when the substrate temperature decreases to 300–350 °C (Fig. 6(c) and (d)). Meanwhile, the resulting carbon nanotip structures are aligned vertically and perpendicular to the substrate surface. The alignment direction is the same as the direction of the DC electrostatic field in the near-substrate area, and is an energetically most favorable orientation of one-dimensional CNSs [9].

Remarkably low substrate temperatures (300–350 °C) sustaining the growth of the carbon nanotip structures can be attributed to the high efficiency of the plasma-surface interactions in high-density inductively coupled plasmas. In addition to high ion densities ($n_i \sim 10^{12}$ cm^{-3}), the LF ICP reactor features very low near-substrate sheath potentials, which make it possible to efficiently control the ion fluxes on the substrate by the DC bias [14]. Our estimates show that in the pressure range of interest here the mean free path of the CH_3 radicals and the near-substrate sheath width are approximately 2 and 1 mm, respectively. Hence, the sheath is nearly collisionless, which is in contrast with the case reported for lower-density plasmas [15]. In this case, the bias-controlled cation fluxes onto the substrate are very strong and can exceed the diffusion fluxes of the neutrals due to near-substrate density gradients. On the other hand, a substantial dilution of methane (partial pressure 1.05 Pa) in argon (partial pressure 7.9 Pa) enhances the physical sputtering effects.

5. Conclusion

We have reported on the LFICP-assisted self-assembly and field emission properties of the carbon nanotip structures on the externally heated Ni-based catalyst layer. A remarkable minimization (up to 300–350 °C) of the growth temperatures can be attributed to outstanding properties of high-density inductively coupled plasmas. In this temperature range, the amorphous carbon phase is suppressed and the self-assembly of the CNTP structures enhanced. However, higher densities of the resulting nanostructures in this substrate temperature range adversely affect the electron field emission properties of the films. To this end, the best EFE have been achieved from the films synthesized under higher substrate temperatures. It is remarkable that the shape, size, surface density, alignment, and uniformity of CNTPs can be efficiently controlled by the substrate temperature and DC bias.

We emphasize that the CNTP growth technique of interest here is a further contribution to the ultimate self-assembly nanotechnology concept and bring in a refreshing enthusiasm in the use of the plasma-based methods for the nano-fabrication processes. One of the apparent present challenges in this direction is to achieve a reasonable degree of positional control and ordering both in the growth plane and growth directions without the use of expensive substrate patterning and nano-lithography processes. Finally, the plasma-assisted self-assembly of the ordered arrays of carbon nanotips with high aspect ratio would be beneficial for the development of the efficient electron field emitters.

Acknowledgements

The authors thank V. Ligatchev for fruitful discussions and anonymous referees for the valuable and stimulating criticisms and comments. Technical assistance of the members of PSAC team is kindly appreciated. This work was partially supported by the Agency for Science, Technology, and Research of Singapore (project 012-101-0024) and the Australian Research Council.

References

[1] S. Iijima, Nature 354 (1991) 56.
[2] M.S. Dresselhaus, G. Dresselhaus, P.C. Eklund, Science of Fullerenes and Carbon Nanotubes, Academic Press, San Diego, 1996.
[3] C. Journet, W.K. Maser, P. Bernier, A. Loiseau, M. Lamy de la Chapelle, S. Lefrant, P. Deniard, R. Lee, J.E. Fisher, Nature 388 (1997) 756.
[4] K. Tanaka, T. Yamabe, K. Fukui (Eds.), The Science and Technology of Carbon Nanotubes, Elsevier, Amsterdam, 1999.
[5] E.T. Thostenson, Z. Ren, T.W. Chou, Compos. Sci. Technol. 61 (2001) 1899.
[6] L. Nilsson, O. Groening, O. Kuettel, P. Groening, L. Schlapbach, J. Vac. Sci. Technol. 20 (2002) 326.
[7] S. Fan, M. Chapline, N.R. Franklin, T.W. Tombler, A.M. Cassell, H. Dai, Science 283 (1999) 512.
[8] C.L. Tsai, C.W. Chao, C.L. Lee, H.C. Shih, Appl. Phys. Lett. 74 (1999) 3462.

[9] C. Bower, W. Zhu, S. Jin, O. Zhou, Appl. Phys. Lett. 77 (2000) 830.
[10] M. Chhowalla, K.B.K. Teo, C. Ducati, N.L. Rupersinghe, G.A.J. Amaratunga, A.C. Ferrari, D. Roy, J. Robertson, W.I. Milne, J. Appl. Phys. 90 (2001) 5308.
[11] C.L. Tsai, C.F. Chen, L.K. Wu, Appl. Phys. Lett. 81 (2002) 721.
[12] L. Delzeit, I. McAnich, B.A. Cruden, D. Hash, B. Chen, J. Han, M. Meyyappan, J. Appl. Phys. 91 (2002) 9.
[13] K.B.K. Teo, M. Chhowalla, G.A.J. Amaratunga, W.I. Milne, D.G. Hasko, G. Pirio, P. Legagneux, F. Wyczisk, D. Pribat, Appl. Phys. Lett. 79 (2001) 1534.
[14] S. Xu, K.N. Ostrikov, Y.A. Li, E.L. Tsakadze, I.R. Jones, Phys. Plasmas 8 (2001) 2459.
[15] Y. Shiratori, H. Hiraoka, Y. Takeuchi, M. Yamamoto, Appl. Phys. Lett. 82 (2003) 2485.
[16] D. Reznik, C.H. Olk, D.A. Neumann, J.R.D. Copley, Phys. Rev., B 52 (1995) 116.
[17] A. Ilie, A.C. Ferrari, T. Yagi, S.E. Rodil, J. Robertson, E. Barborini, P. Milani, J. Appl. Phys. 90 (2001) 2024.
[18] J.W. Ager III, D.K. Veirs, G.M. Rosenblatt, Phys. Rev., B 43 (8) (1991) 6491.
[19] V. Ligatchev, Physica. B 337 (2003) 333.
[20] Y.J. Li, Z. Sun, S.P. Lau, G.Y. Chen, B.K. Tay, Appl. Phys. Lett. 79 (11) (2001) 1670.
[21] K.B.K. Teo, M. Chhowalla, G.A.J. Amaratunga, W.I. Milne, G. Pirio, P. Legagneux, F. Wyczisk, D. Pribat, D.G. Hasko, Appl. Phys. Lett. 80 (11) (2002) 2011.
[22] E. Kovacevic, I. Stefanovic, J. Berndt, J. Winter, J. Appl. Phys. 93 (2003) 2924.
[23] S.V. Vladimirov, K. Ostrikov, Phys. Rep. 393 (2004) 175.
[24] G. Viera, M. Mikikian, E. Bertran, P.R. Cabarrocas, L. Boufendi, J. Appl. Phys. 92 (2002) 4684.
[25] J. Perrin, M. Shiratani, P. Kae-Nune, H. Videlot, J. Jolly, J. Guillion, J. Vac. Sci. Technol. 16 (1998) 278.